

## Supplemental Information

### Hyperpolarized [1-<sup>13</sup>C]Pyruvate-to-[1-<sup>13</sup>C]Lactate Conversion is Rate Limited by Monocarboxylate Transporter-1 in the Plasma Membrane

Yi Rao<sup>1</sup>, Seth Gammon<sup>1</sup>, Niki M Zacharias<sup>2</sup>, Tracy Liu<sup>1</sup>, Travis Salzillo<sup>1</sup>, Yuanxin Xi<sup>3</sup>,  
Jing Wang<sup>3</sup>, Pratip Bhattacharya<sup>1</sup>, David Piwnica-Worms<sup>1,4</sup>

<sup>1</sup>Department of Cancer System Imaging, <sup>2</sup>Department of Urology, <sup>3</sup>Department of Biostatistics, University of Texas M.D. Anderson Cancer Center, Houston, TX 77030

**Keywords:** MCT1, cancer metabolism, hyperpolarized <sup>13</sup>C, <sup>13</sup>C magnetic resonance spectroscopy, non-invasive biomarkers

**Running Title:** MCT1 Limits Hyperpolarized [1-<sup>13</sup>C]Pyruvate Metabolic Conversion Rates

No COI declared.

**Financial Support:** P50 CA94056, UT STARs Award, P30 CA016672, Pancreatic Cancer Action Network (16-65-BHAT), CPRIT Research Training Grant Award (RP170067), and a generous gift from the Estate of Barbara Cox Anthony/Koch Foundation.

<sup>4</sup>Corresponding author:

David Piwnica-Worms, M.D., PhD.,  
Department of Cancer Systems Imaging,  
The University of Texas M.D. Anderson Cancer Center,  
1400 Pressler Street, Unit 1479  
FCT16.6030, Houston, Texas, 77030  
Tel: 713-745-0850  
Fax: 713-745-7540  
Email: [dpiwnica-worms@mdanderson.org](mailto:dpiwnica-worms@mdanderson.org)

**This PDF file includes:**

Supplementary text: Methods

Figures S1 to S7

## Detailed Methods

### *Cell culture and cell lines*

Mia Paca-2, MDA-MB-231, Panc03.27, and hTERT-HPNE cells were obtained from the American Type Culture Collection (ATCC, Manassas, VA). QGP1 was purchased from the Japanese Collection of Research Bioresources (JCRB, Japan) cell bank. All cells tested negative for mycoplasma infection, and were maintained based on recommended culturing conditions. Mia Paca-2 and MDA-MB-231 cells were grown in DMEM media with 2 mM glutamine and 10% fetal bovine serum (FBS). Panc 03.27 cells were maintained in RPMI-1640 media supplemented with 10 Units/mL human recombinant insulin and 15% FBS. QGP1 cells were cultured in RPMI-1640 media with 10% FBS. HPNE cells were maintained in 75% DMEM without glucose and 25% Medium M3 Base (Incell Corporation, San Antonio, TX ) supplemented with 2 mM L-glutamine, 1.5 g/L sodium bicarbonate, 5.5 mM D-glucose, 750 ng/mL puromycin, 10 ng/mL human recombinant EGF (Thermo Fisher Scientific, Carlsbad, CA) and 5% FBS. DMEM, DMEM without glucose, RPMI-1640, sodium bicarbonate, and D-glucose were purchased from Sigma Aldrich (Sigma-Aldrich, St. Louis, MO). Cell cultures were maintained at 37 °C in a humidified 5% CO<sub>2</sub> atmosphere.

### *Stable knockdown and overexpression of MCT1*

For stable MCT1 knockdown, Mia Paca-2 and Panc 03.27 cells were seeded at a density of  $5.0 \times 10^4$  cells/well into 24-well plates and allowed to attach for 24 hr. Cells were transduced with SMARTvector inducible human SLC16A1 hEF1a-TurboGFP shRNA lentiviral targeting MCT1 or SMARTvector Inducible Non-targeting Control hEF1a/TurboGFP (Dharmacon, Lafayette, CO). Selection of cells stably expressing Tet-

inducible SLC16A1 hEF1a-TurboGFP shRNA or Control-shRNA started 48 h post-transfection by replacing the growth medium with medium containing 2 µg/mL of puromycin. The puromycin-containing medium was refreshed every 3 days for two weeks to obtain stable cells containing Tet-inducible SLC16A1-shRNA and Control-shRNA. For stable overexpression of MCT1 in QGP1 and Mia Paca-2 MCT1 cells, similar transduction procedures were followed, except Precision LentiORF Human SLC16A1 GFP lentiviral particles or Precision LentiORF RFP Positive Control particles (Dharmacon, Lafayette, CO) were used.

#### *mRNA sequencing*

mRNA was extracted and purified from each cell lines using RNeasy Kit per manufacturer instruction (Qiagen, Germantown, MD). mRNA samples were sequenced using Illumina HighSeq Sequencing platform at MD Anderson Next Generation Sequencing Core. mRNA data was mapped and processed by MD Anderson biostatistics core.

#### *Western blotting*

For whole cell lysate, cells were lysed in Cell Lysis Buffer (Cell Signaling Technology, Danvers, MA), supplemented with protease inhibitor cocktail (Thermo Fisher Scientific, Carlsbad, CA). Membrane and cytoplasmic subcellular fractions were separated using a commercial Cell Fractionation Kit (Cell Signaling Technology, Danvers, MA), supplemented with protease inhibitor cocktail (Thermo Fisher Scientific, Carlsbad, CA) as per the manufacture protocol. Lysate loading was normalized to protein content quantified with the Coomassie Protein Assay (Thermo Fisher Scientific, Carlsbad, CA). Proteins were resolved on 4 – 20% SDS-PAGE gels (BioRad, Hercules, CA) or NuPAGE 4 – 12%

Bio-Tris Protein gels (Thermo Fisher Scientific, Carlsbad, CA), and transferred to Trans-blot Turbo nitrocellulose membranes (BioRad, Hercules, CA). Post-transferred nitrocellulose membranes were stained in Ponceau S staining solution to evaluate total protein loading. For primary antibody-protein hybridization, membranes were probed with the following antibodies at 4°C overnight: MCT1 (Thermo Fisher Scientific, Carlsbad, CA; Lot # TH2617863; TH2585400), MCT2 (Novus Biologicals, Centennial, CO; Lot # C2E170918), MCT4 (Boster, Pleasanton, CA; Lot # 11Q405094), LDHA (R&D System, Minneapolis, MN; Lot# CKJE011708A), Na/K-ATPase (Abcam, Cambridge, MA), and GAPDH (Abcam, Cambridge, MA; BioRad, Hercules, CA). Thereafter, secondary anti-mouse or anti-rabbit horseradish peroxidase-conjugated IgG antibodies (BioRad, Hercules, CA) were incubated for 1 h at room temperature. Protein bands were developed with chemiluminescent reagents (BioRad, Hercules, CA) and imaged with an Azure c600 (Azure Biosystems, CA). Protein bands were quantified by total intensity using NIH ImageJ and normalized to Ponceau S staining (*SI Appendix*, Figure S1) (Abcam, Cambridge, MA).

#### *Real-Time quantitative PCR assays*

RNA was collected in 300 µL TRizol reagent (Thermo Fisher Scientific, Carlsbad, CA) and extracted from Mia Paca-2, Panc 03.27, and QGP1 cells, along with their MCT1 knockdown and overexpression stable cell lines with the Direct-zol™ RNA Kit (Zymo Research, Irvine, CA). The amount of RNA from each sample was quantified using a Nanodrop 1000 (Thermo Fisher Scientific, Carlsbad, CA). cDNA was synthesized using Maxima First Strand cDNA Synthesis Kit for RT-qPCR (Thermo Fisher Scientific, Carlsbad, CA). Real-time quantitative PCR was performed with primers for MCT1

(forward: 5-AGGTCCAGTTGGATACACCCC-3 and reverse: 5-GCATAAGAGAAGCCGATGGAAAT-3) and glyceraldehyde-3-phosphate dehydrogenase (GAPDH) (forward: 5- ATGGGGAAGGTGAAGGTCG-3 and reverse: 5-TAAAAGCAGCCCTGGTGACC3) (Sigma-Aldrich, St. Louis, MO). DNA amplification was quantified with SYBR green (BioRad, Hercules, CA) on a CFX96 Touch Real-Time PCR Detection System (BioRad, Hercules, CA). Expression of target gene mRNA relative to reference gene mRNA (GAPDH) was calculated using the Bio-Rad CFX Manager (BioRad, Hercules, CA), and statistical analysis was done using the GraphPad Prism 7.01. Assays were performed in triplicate from three independent experiments.

#### *In vitro* analysis of extracellular acidification rate (ECAR)

The Seahorse XF glycolysis stress assay was used to measure the extracellular acidification rate (ECAR). Five different cell lines were seeded on XF96 Cell Culture Microplates (Seahorse Bioscience, Billerica, MA) in their original growth media 48 h before the experiment at the following cell densities:  $1.2 \times 10^4$  Mia Paca-2,  $1.5 \times 10^4$  Panc 03.27,  $2.0 \times 10^4$  QGP1,  $1.5 \times 10^4$  MDA-MB-231, and  $1.5 \times 10^4$  HPNE. For the Seahorse assay, cells were washed and maintained with DMEM lacking  $\text{NaHCO}_3$ , supplemented with 2 mM glutamine with 5 mM glucose, and adjusted to pH 7.4. Experiments were performed with an XF96 analyzer, and baseline ECARs were normalized to cellular DNA stained with Hoechst 33342 (Thermo Fisher Scientific, Carlsbad, CA) imaged by an Operetta High-Content Imaging System (PerkinElmer, MA). Measured baseline ECAR data in the cell panel were normalized to Panc03.27 values. Data were analyzed with GraphPad Prism 7.01. Each experiment was performed in quintuplicate and repeated three independent times.

### *Pyruvate or lactate content and pyruvate influx assay*

Cells were seeded at a density of  $2.0 \times 10^4$  cells/well into 96-well black wall clear bottom plates. Doxycycline-inducible cell lines were supplemented with 500 ng/ml doxycycline for 48 hr. On the day of the experiment, after a wash with 100  $\mu$ L of PBS, cells were incubated in 100  $\mu$ L of DMEM media containing 0 or 10 mM sodium pyruvate for 6 seconds at 37°C. Thereafter, cells were quickly washed 3 times with ice-cold PBS, and lysed with 50  $\mu$ L of Pyruvate Assay Buffer or Lactate Assay Buffer plus 50  $\mu$ L of the Master Reaction Mix prepared from a Pyruvate Assay Kit or Lactate Assay Kit (Sigma-Aldrich, St. Louis, MO). After 30 min of incubation at room temperature, the fluorescence intensity ( $\lambda_{\text{ex}} = 535/\lambda_{\text{em}} = 587$  nm) was measured with a Synergy H4 microplate reader (BioTek, Winooski, VT); the fluorescence intensity correlated with cellular pyruvate or lactate content. The difference in cell pyruvate content between incubation in baseline (0) or 10 mM sodium pyruvate media was used to calculate unidirectional pyruvate influx. Calculated pyruvate or lactate content and influx data were normalized to cellular DNA as stained with Hoechst 33342 (Thermo Fisher Scientific)

### *LDHA activity assay*

Cells were washed with ice-cold PBS and then lysed in ice-cold LDHA Assay Lysis Buffer (Sigma-Aldrich, St. Louis, MO). Protein content was quantified with the Coomassie Protein Assay. For each well of a 96 well plate, 25  $\mu$ L of cell-extracted LDHA, 125  $\mu$ L of Tris/NaCl/NADH buffer, and 25  $\mu$ L of Tris/NaCl/pyruvate with various pyruvate concentrations were added. Reduced NADH absorbs light at 340 nm, whereas oxidized NAD<sup>+</sup> does not. Therefore, to quantify the enzymatic activity of LDHA, the change of absorbance at 340 nm due to NADH oxidation was measured using a Synergy H4

microplate reader (BioTek, Winooski, VT). The Synergy H4 microplate reader was programmed to shake the microplate for 30 seconds, and read absorbance of NADH at 340 nm five times with 30 second intervals. Data were analyzed with GraphPad Prism 7.01. Experiments were performed in triplicate and repeated three independent times.

#### *NAD<sup>+</sup>/NADH assay*

Cells with/without doxycycline treatment were seeded at a density of  $5.0 \times 10^4$  cells/well into 96-well black wall clear bottom plates and allowed to attach overnight. On the next day, cells were washed with PBS, and lysed in 100  $\mu$ l of PBS + 1% DTAB base solution (1:1). Then, each 100  $\mu$ l sample was equally split into two wells, one for NAD<sup>+</sup> measurement and one for NADH measurement. The NAD/NADH-Glo Assay was then used to assess NAD<sup>+</sup> and NADH levels per kit instructions (Promega, Madison, WI). After 60 min of incubation at room temperature, a bioluminescence signal was measured with a Synergy H4 microplate reader (BioTek, Winooski, VT). The bioluminescence signal correlated with NAD<sup>+</sup> or NADH content.

#### *Cell encapsulation*

Cells grown in T175 flasks were trypsinized, washed, and resuspended in 2.7% w/v alginate (Sigma-Aldrich, St. Louis, MO) in Hanks BSS solution (Sigma-Aldrich, St. Louis, MO). An alginate mixture containing  $2.5 \times 10^7$  cells was then transferred into a 1 mL syringe. A 24G3/4 catheter (Braun, Kronbergim Taunus, Germany) with a 23G3/4 needle inserted through the base was connected to the syringe (*SI Appendix*, Figure S2). The syringe was clamped onto a syringe pump (Harvard Apparatus, Holliston, MA) and a flask with 100 mL of 150 mM CaCl<sub>2</sub> and 0.09% NaCl w/v solution was placed underneath the



needle. A ground electrode was clipped to the needle piercing the catheter, and the other electrode was submerged in the CaCl<sub>2</sub> solution. A 5 kV voltage was applied between the needle and the CaCl<sub>2</sub> solution, and upon syringe pump actuation, cell-encapsulated alginate beads were formed upon passage through to the electromagnetic field, and stabilized by crosslinking induced by the CaCl<sub>2</sub> solution. Thereafter, beads were washed in growth medium and transferred into a petri dish containing cell-appropriate growth medium. Cell-encapsulated alginate microbeads were maintained at 37°C in a humidified 5% CO<sub>2</sub> incubator overnight for subsequent *in vitro* hyperpolarization experiments performed the next day.

#### *Diffusion-weighted MRI*

[<sup>1</sup>H] magnetic resonance imaging (MRI) was performed using a 7 T Bruker Biospec MR system, with BGA-12 gradients. A <sup>1</sup>H volume coil with 35 mm inner diameter (Bruker, MA) was used for proton imaging. A 5mL conical tube filled with either water, hyperpolarization medium alone, or 25% or 90% alginate beads by volume in hyperpolarization medium was mixed by inverting, and immediately placed in the center of the <sup>1</sup>H volume coil. The position of the tube was confirmed using a 3-plane fast low-angle shot (FLASH) gradient-echo sequence (TE=3.6 ms, TR=100 ms). A standard diffusion measurement (spin-echo) was run on all phantoms with a field of view 3 x 3 cm, 128 x 96 matrix, and 8 axial slices of 1 mm thickness, TE=30.758 ms, TR= 900 ms, bandwidth 50 kHz, 1 average. DW data were acquired with b = 233, 435, 636, 837, 1037, 2040, and 4272 sec/mm<sup>2</sup>, d = 1, and processed using the Image Sequence Analysis Tool in Paravision 6.0.1. A non-linear regression model was used to curve-fit the T2 signal and various b values to determine bulk ADC values. The standard deviation of the fitting represented the

deviation between measured values compared to best-fit values. The extra sum-of-squares F-test was used to compare the non-linear curve-fit between various concentrations of alginate beads, cell-encapsulated alginate beads, and medium alone using GraphPad Prism 8.0.0. Because the DWI experiments were performed on a 7T MR imaging system, we attributed the apparent difference in baseline proton signal at  $b = 0$  to differences in the position of the conical tube within the field and coil from experiment to experiment rather than differences in the size of water compartments. Only the slope is relevant to calculation of bulk ADC values.

#### *In vitro hyperpolarization experiments using vertical bore NMR*

Cell-encapsulated alginate beads (1 mL) made the prior day were washed and resuspended in 2.5 mL of assay medium consisting of phenol red-free DMEM medium supplemented with 2 mM glutamine, 5 mM glucose, 20% (v/v) deuterium oxide ( $D_2O$ ) (Sigma-Aldrich, St. Louis, MO), and 15 mM HEPES buffer. Cell/bead suspensions were then transferred into a 10 mm screw-cap NMR tube (Wilmad-LabGlass, Vineland, NJ) that was fitted with tubing and an injection port for quick delivery of hyperpolarized material. Experiments were conducted in a 7 T Bruker BioSpin NMR spectrometer (Billerica, MA) with a 10 mm broadband probe and running TopSpin 3.5 software. NMR tubes containing cell-encapsulated alginate beads were equilibrated in the NMR spectrometer at 37°C prior to hyperpolarized  $[1-^{13}C]$ pyruvate injection. For analysis, an aliquot of 26.5 mg of a pyruvic acid mix containing  $[1-^{13}C]$ pyruvic acid (Isotec, Sigma-Aldrich, St. Louis, MO), with 15 mM Trityl OX063 polarizing radicals (Oxford instrument, Abingdon, UK) and 1.5 mM Dotarem (Guerbet, France) was polarized in a HyperSense DNP system (Oxford Instruments, UK) with a 3.35 T magnetic field for ~30 minutes at

1.40 K with a microwave irradiation frequency of 96.136 GHz, similar to published procedures (1). The frozen hyperpolarized [1-<sup>13</sup>C]pyruvic acid was then dissolved in 4 mL of the dissolution medium containing 40 mM Trizma Pre-Set Crystals at pH 7.6 (Sigma-Aldrich, St. Louis, MO), 80 mM sodium hydroxide, 0.1 g/L disodium EDTA dihydrate, and 50 mM sodium chloride at 180°C. The hyperpolarized [1-<sup>13</sup>C]pyruvic acid dissolution was further diluted into a specialized hyperpolarization buffer medium comprising modified DMEM supplemented with 2 mM glutamine, 5 mM glucose, and 25 mM HEPES buffer (2 parts:1 part), which was developed to ensure a physiologically balanced osmolality and pH buffering capacity. Thus, the hyperpolarized [1-<sup>13</sup>C]pyruvic acid stock was 37.7 mM. At time zero of acquisition, 500 µl of the hyperpolarized [1-<sup>13</sup>C]pyruvic acid stock was injected into the NMR tube (containing 2.5 ml of buffering medium and 1 ml of alginate/cell beads). The final concentration of [1-<sup>13</sup>C]pyruvic acid in the experiment was ~ 4.7 mM. Single consecutive <sup>13</sup>C scans were taken using Waltz decoupling (zgdc pulse) every 6 seconds with 15° flip angle for 3 minutes. Acquired NMR spectra were phased and baseline corrected, referenced, and the signal intensities of hyperpolarized [1-<sup>13</sup>C]pyruvate (~173 ± 1 ppm) and [1-<sup>13</sup>C]lactate (~185 ± 1 ppm) spectra were integrated using MestReNova 10.0 software (MestreLab Research, CA). After NMR spectra acquisition, samples of cell-encapsulated alginate beads were then subjected to Alamar Blue Assay (Thermo Fisher Scientific, Carlsbad, CA) to confirm cell viability except for the digitonin-treated permeabilized samples. Initial hyperpolarized [1-<sup>13</sup>C]pyruvate-to-[1-<sup>13</sup>C]lactate conversion rate =  $\frac{\text{Sum}([1-^{13}\text{C}]lactate)(6-18\text{ s})}{\text{Sum}([1-^{13}\text{C}]pyruvate)(6-18\text{ s})}$ . Total hyperpolarized [1-<sup>13</sup>C]pyruvate-to-[1-<sup>13</sup>C]lactate conversion =  $\frac{\text{Sum}([1-^{13}\text{C}]lactate)(0-198\text{ s})}{\text{Sum}([1-^{13}\text{C}]pyruvate)(0-198\text{ s})}$ .

### *Xenografts tumor models*

Animal experiments were performed in compliance with protocols approved by the Institutional Animal Care and Use Committee of the MD Anderson Cancer Center. To establish tumor xenografts, an aliquot of 50  $\mu$ l DMEM and Matrigel (BD Bioscience, San Jose, CA) mix (1:1 ratio) containing  $2 \times 10^6$  Mia Paca-2 doxycycline-inducible MCT1 knockdown cells or Mia Paca-2 doxycycline-inducible NTC cells were injected subcutaneously into the right hind legs of 8 – 12 week-old female athymic C57BL/6-nu/nu mice (Charles River Laboratories, Wilmington, MA). Tumor volumes were measured every 7 days with a caliper, and calculated as  $\text{width}^2 \times \text{length} / 2$ . When tumor volumes reached  $\sim 250 \text{ mm}^3$ , mice from paired groups were subjected to pre-doxycycline MRI/hyperpolarized  $[1-^{13}\text{C}]$ pyruvic acid MRS. Immediately after the imaging session, paired groups of mice were supplemented with freshly dissolved doxycycline (1 mg/mL in 5% sucrose water) for  $\sim 7 - 14$  days to induce MCT1 knockdown or NTC expression. Post-doxycycline, MRI/hyperpolarized  $[1-^{13}\text{C}]$ pyruvic acid MRS experiments were performed on the same animal. Upon completion of imaging, mice were sacrificed, and tumors were harvested for immunohistochemical analysis.

### *In vivo hyperpolarization experiments using MRS*

$[^1\text{H}]$  magnetic resonance imaging (MRI) was performed using a 7 T Bruker Biospec small animal MR system, with BGA-12 gradients. A  $^1\text{H}$  volume coil with 72 mm inner diameter (Bruker, MA) was used for proton imaging. Concurrently, hyperpolarized  $[1-^{13}\text{C}]$ pyruvic acid magnetic resonance spectra were measured using a  $^{13}\text{C}$  Doty Scientific (Columbia, South Carolina) transmit/receive surface coil placed over the established tumor. Before imaging, animals were anesthetized with 1 – 2% isoflurane and placed on a water-heated

imaging sled. Respiratory and heart rates of the animals were monitored during experiments. An 8 M  $^{13}\text{C}$ -urea capillary phantom was placed above the surface coil for chemical shift referencing (2). Animal positioning was confirmed using a 3-plane fast low-angle shot (FLASH) gradient-echo sequence (TE = 3.6 ms, TR = 100 ms). The tumor location was observed in T2-weighted axial and coronal spin-echo images (TE = 50 ms, TR = 2500 ms, with echo train length of 10, 2 cm  $\times$  2 cm FOV, and 1 mm slice thickness). For  $^{13}\text{C}$  spectroscopy measurements, the  $^{13}\text{C}$  channel was tuned, and set to acquire  $^{13}\text{C}$  signal every 2 s for 3 min using a slice-selective pulse-acquire sequence (TE = 2.4 ms, TR = 2 s, 20° excitation angle, 2048 points acquired over a 4.96 kHz bandwidth). Similar to *in vitro* hyperpolarization experiments, the [1- $^{13}\text{C}$ ]pyruvate acid was dissolved in 4 ml of the dissolution medium containing 40 mM Trizma Pre-Set Crystals at pH 7.6 (Sigma-Aldrich, St. Louis, MO), 80 mM sodium hydroxide, 0.1 g/L disodium EDTA dihydrate, and 50 mM sodium chloride at 180°C. The acquisition was initiated approximately 15 seconds prior to injection of 200  $\mu\text{l}$  of ~60 mM hyperpolarized [1- $^{13}\text{C}$ ]pyruvic acid solution via tail vein bolus injection. The majority of [1- $^{13}\text{C}$ ]pyruvic acid mixtures were polarized using a HyperSense DNP system (Oxford Instruments, UK), the same as described in *In vitro hyperpolarization experiments using vertical bore NMR*, while a few hyperpolarized [1- $^{13}\text{C}$ ]pyruvic acid mixtures were polarized in a SPINlab system (General Electric, Boston, MA). The acquired spectra were phase and baseline corrected, referenced, and integrated using MestReNova 10.0 software (MestreLab Research, CA). Above baseline hyperpolarized [1- $^{13}\text{C}$ ]pyruvate-to-[1- $^{13}\text{C}$ ]lactate conversion =

$$\frac{\text{Sum}([1-^{13}\text{C}]\text{lactate})(\text{above baseline})}{\text{Sum}([1-^{13}\text{C}]\text{pyruvate})(\text{above baseline})}$$

### *Survival analysis*

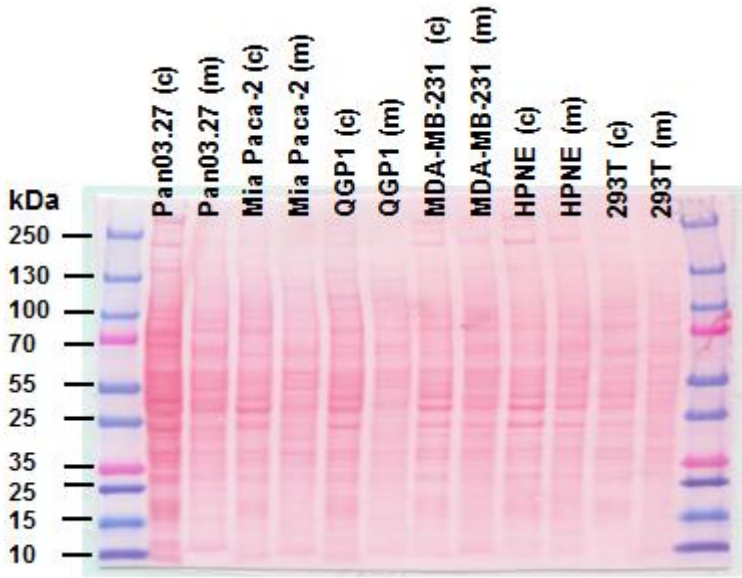
Datasets from the Human Protein Atlas (HPA) were used to compare mRNA expression of MCTs between normal and cancer tissues. Furthermore, datasets from the HPA were also used for determining overall survival of patients with pancreatic cancer, renal cancer, lung cancer, and cervical cancer. Gehan-Breslow-Wilcoxon and Log-rank tests were used to estimate  $p$ -values between high and low expression groups (using top and bottom 25% as the cutoff for grouping). Chi-square tests were used to test the association between two gene expression profiles with high (>75%), medium (< 75% – >25%), and low (< 25%) expression levels for the entire cohort of each cancer type. A two-tailed,  $t$ -test with a  $p$  value < 0.05 was considered significant. Analyses were performed using R 3.2.3.

### *Statistical analysis*

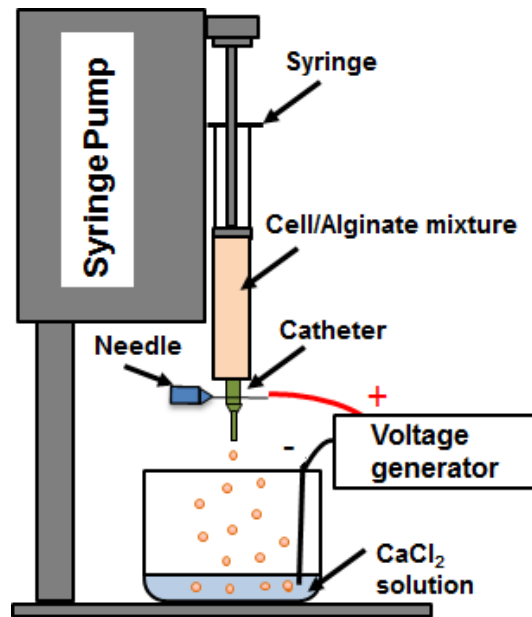
For normalization analysis, cellular data were normalized to Panc03.27 values across the cell panel. The Pearson test was used to assess the correlation between normalized ECAR, LDHA protein content, LDHA total activity, baseline pyruvate cell content, pyruvate influx, or protein content of MCTs with initial [1-<sup>13</sup>C]pyruvate-to-[1-<sup>13</sup>C]lactate conversion rates across the panel of cell lines, and the likelihood ratio test  $p$ -values were reported. A paired  $t$ -test was used to evaluate the difference between paired initial [1-<sup>13</sup>C]pyruvate-to-[1-<sup>13</sup>C]lactate conversion rates both *in cellulo* and *in vivo*, and the likelihood ratio test  $p$ -values were reported.

### *Data Availability*

All relevant data are within the manuscript and its SI Appendix files.

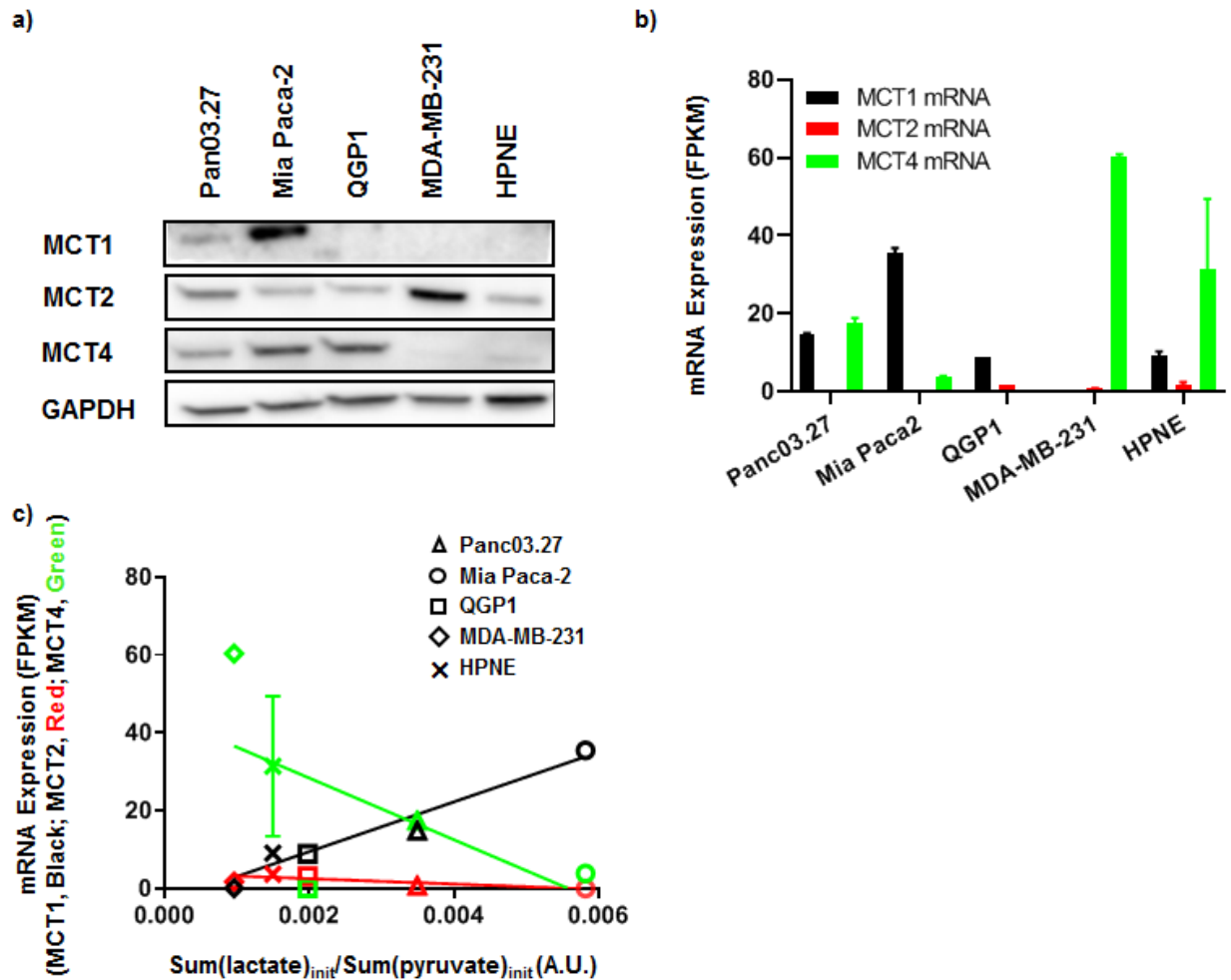


**Figure S1.** Protein loading contents stained with Ponceau S across the cell panel for membrane protein content normalization.

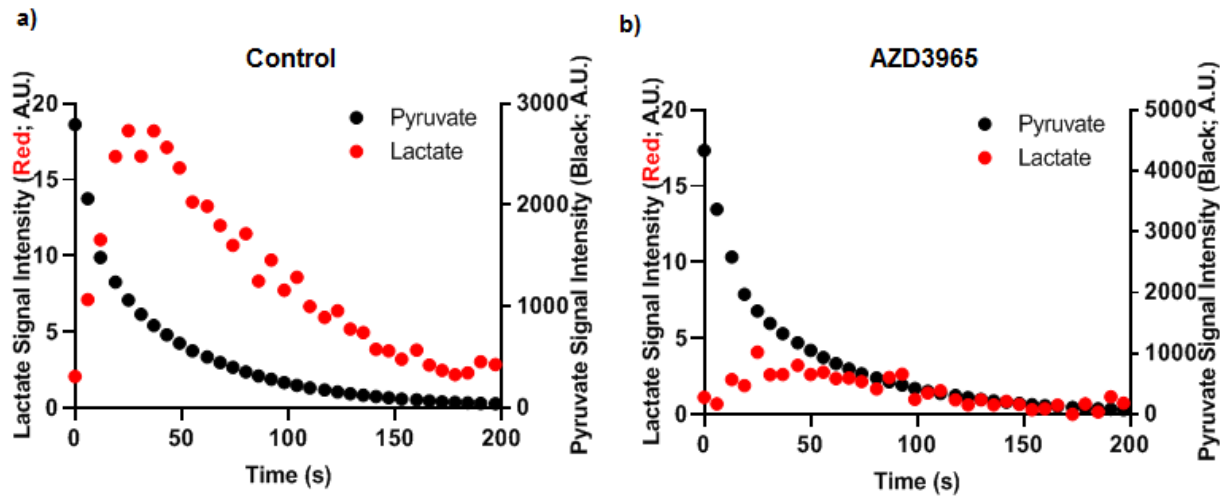


**Figure S2.** Schematic for fabrication of cell-encapsulated alginate beads.

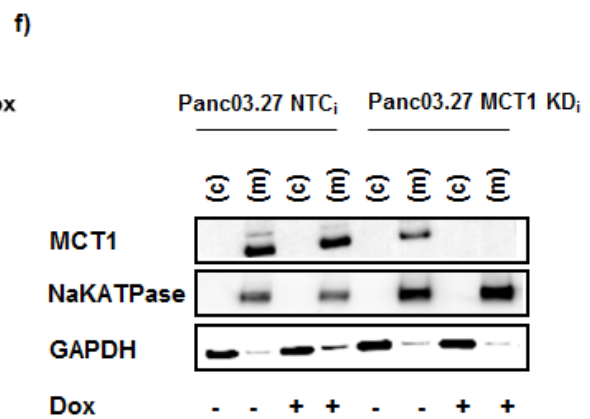
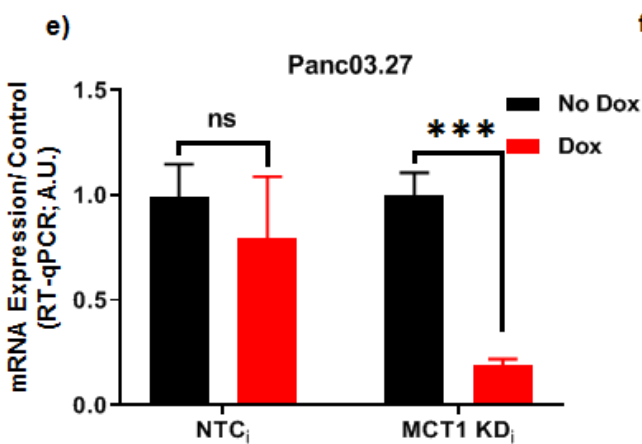
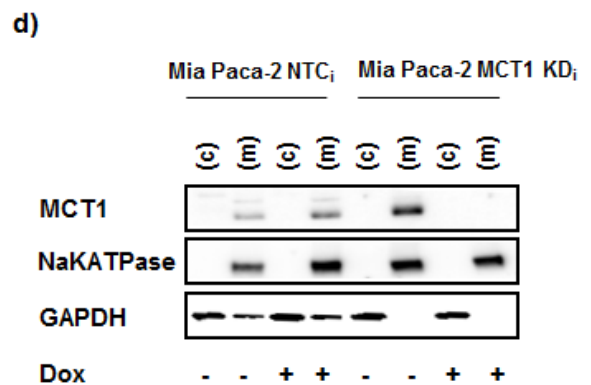
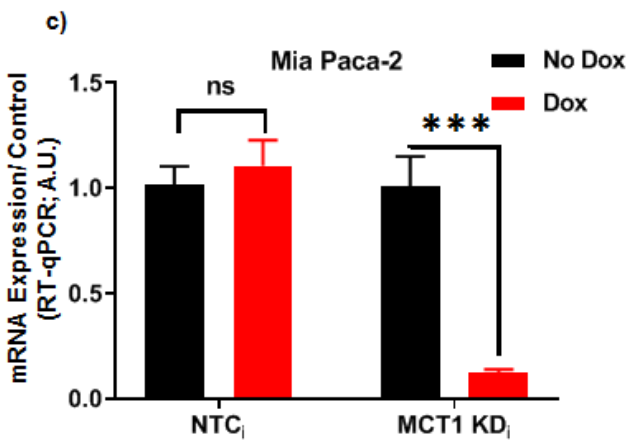
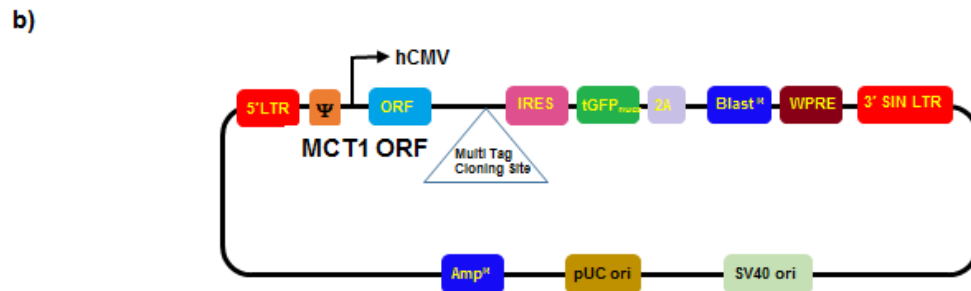
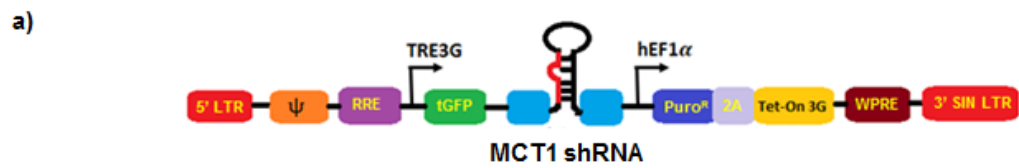


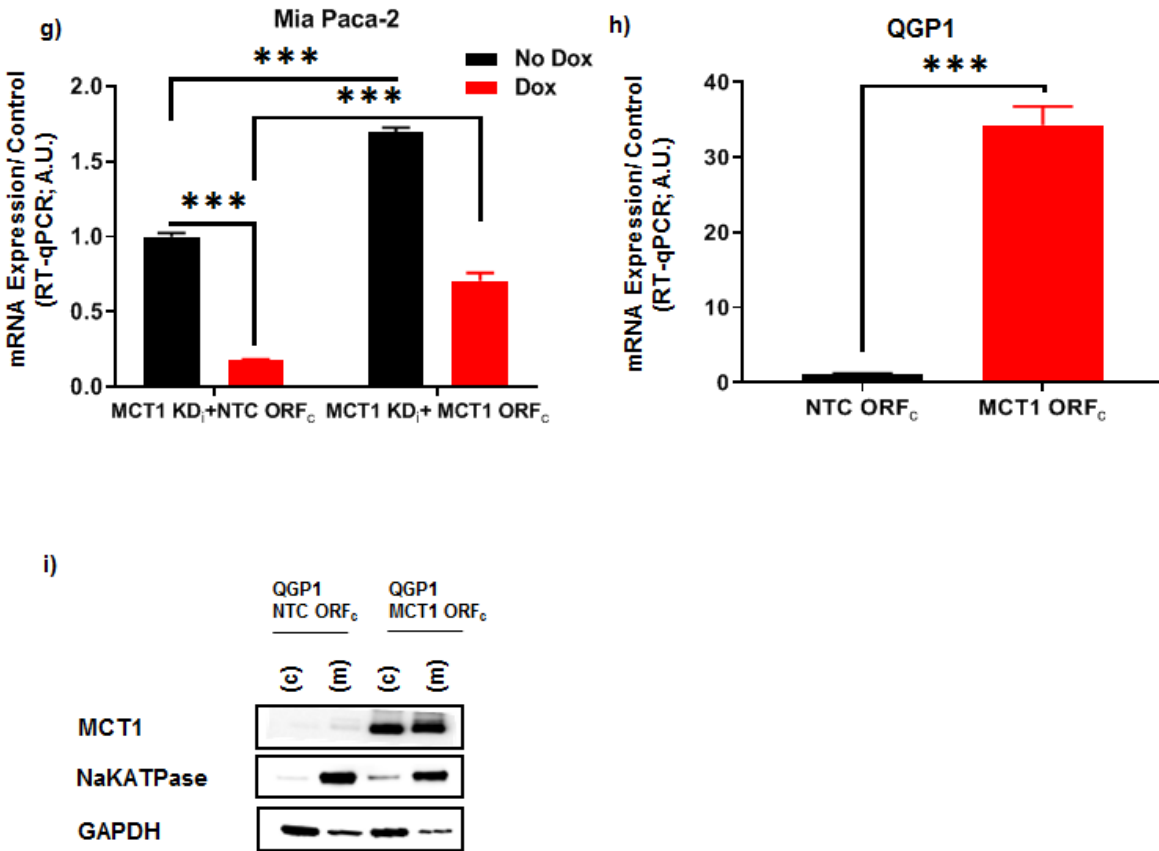


**Figure S3.** a) Western blot of MCTs in whole cell lysates across the cell panel. b) mRNA expression profile in fragments per kilobase of transcript per million mapped reads (FPKM) across the cell panel. c) Pearson correlation analysis between initial hyperpolarized  $[1-^{13}\text{C}]$ pyruvate-to- $[1-^{13}\text{C}]$ lactate conversion rates and mRNA expression of MCT1, 2, or 4;  $r_{(\text{MCT1})} = 0.98$ ,  $p = 0.004$ ;  $r_{(\text{MCT2})} = -0.78$ ,  $p = 0.12$ ;  $r_{(\text{MCT4})} = -0.64$ ,  $p = 0.24$ .



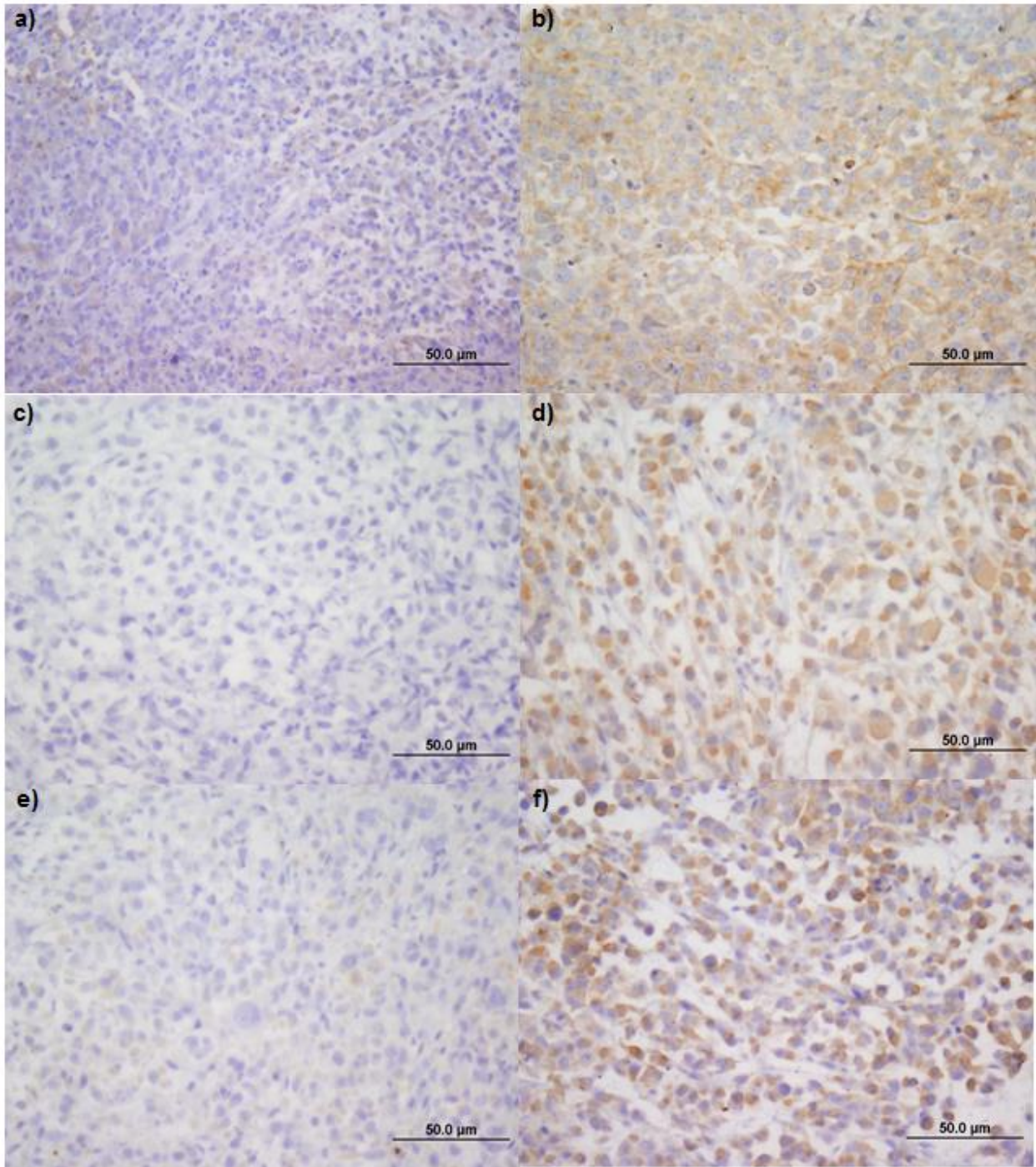
**Figure S4.** Hyperpolarized  $[1-^{13}\text{C}]$ pyruvate and  $[1-^{13}\text{C}]$ lactate spectra over time in response to pharmacological inhibition of MCT1 with  $0.5\ \mu\text{M}$  AZD3965 in Mia Paca-2 cells. Pyruvate (black), Lactate (red). a) Drug-free control. b)  $0.5\ \mu\text{M}$  AZD3965 treated.



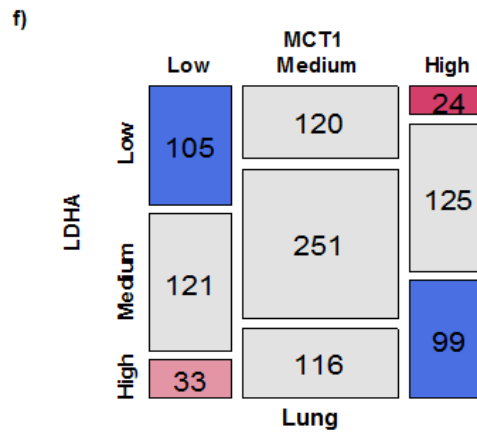
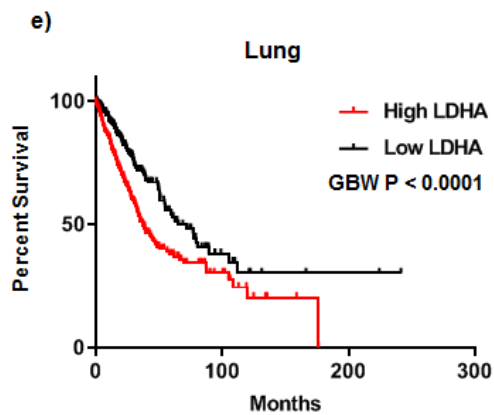
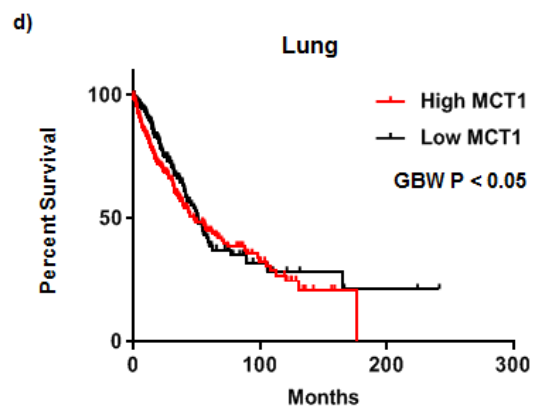
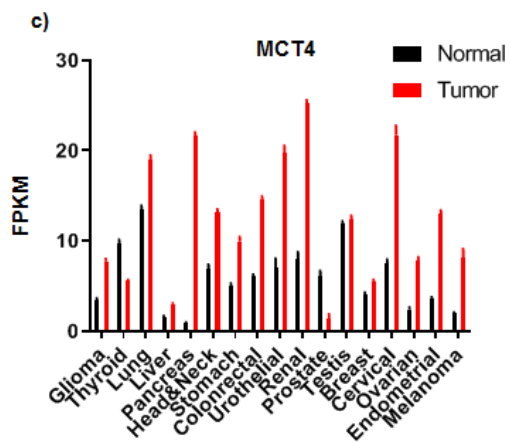
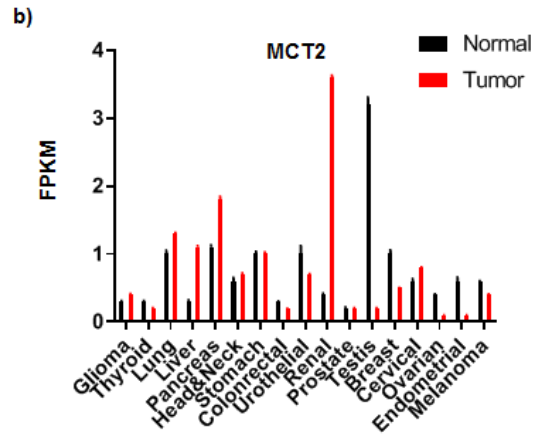
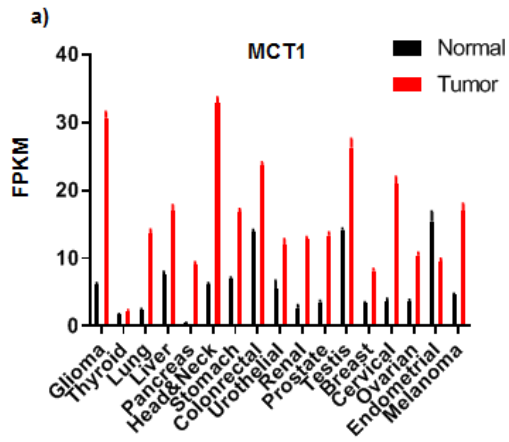


**Figure S5.** Generating stable cell lines with doxycycline-inducible MCT1 knockdown sequence (MCT1 KD<sub>i</sub>) or constitutive overexpressing MCT1 ORF<sub>c</sub> sequences (MCT1 ORF<sub>c</sub>). a) Doxycycline-inducible lentiviral shRNA vector utilizing the Tet-on 3G bipartite system (image adapted from Dharmacon, Inc.). b) Constitutive MCT1-overexpressing ORF system (image adapted from Dharmacon, Inc.). c-i) Doxycycline-inducible MCT1 knockdown or constitutive overexpression of MCT1 in stable cell lines evaluated at either transcriptional or protein levels using RT-qPCR or Western blot, respectively. NaK-ATPase was a biomarker for membrane protein enrichment, while GAPDH served as a marker of cytosol. c & d) Mia Paca-2 MCT1 KD<sub>i</sub> stable cell line compared to its NTC<sub>i</sub> control. e & f) Panc03.27 MCT1 KD<sub>i</sub> stable cell line compared to its NTC<sub>i</sub> control. g) MCT1 mRNA expression in Mia Paca2 doxycycline-inducible stable cell line (Mia Paca-2 MCT1

KDi) containing a NTC ORF<sub>c</sub> or MCT1 ORF<sub>c</sub>. h & i) MCT1 mRNA expression and Western blot for QGP1 MCT1 ORF<sub>c</sub> stable cells compared to its NTC ORF<sub>c</sub> control. Error bars represent, S.D. \*\*\*,  $p < 0.01$ , paired  $t$ -test.



**Figure S6.** a-f) Representative immunohistochemistry (IHC) staining for MCT1 from Mia Paca-2 xenograft tumors. All tumor sections were stained with H&E. a, c, e) Mia Paca-2 MCT1 KD tumors post doxycycline induction. b, d, f) Mia Paca-2 NTC tumors post doxycycline induction.



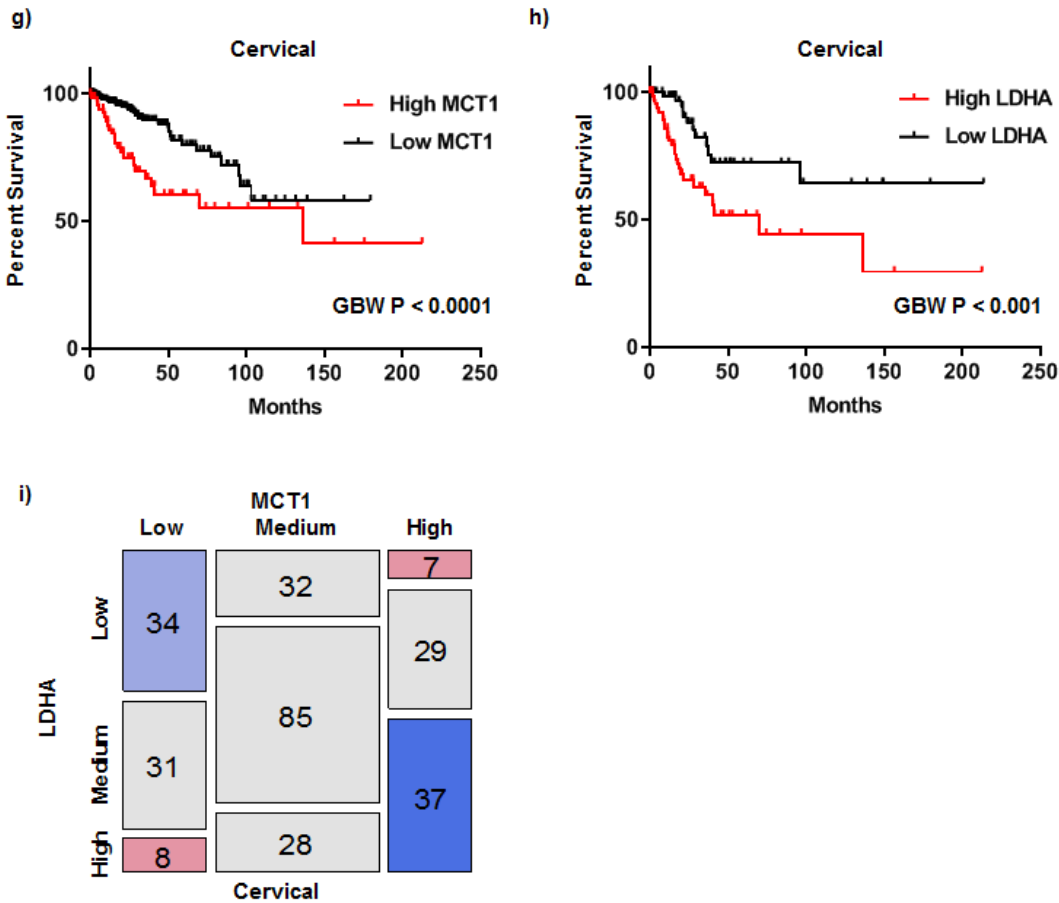


**Figure S7.** Expression profiles of MCT family members, MCT1, 2, and 4 across various tissues between normal individuals and cancer patients. a–c) Expression profiles of MCT1 (a), MCT2 (b), and MCT4 (c) between cancer and normal tissues. d–i) mRNA expression profiles of MCT1 or LDHA correlated with overall patient survival in lung and cervical cancers. Gehan-Breslow-Wilcoxon tests were used to estimate the  $p$ -values between high and low expression groups (using top and bottom 25% as the cutoff for grouping). Pearson Chi-square tests were used to estimate the  $p$ -values between MCT1 and LDHA expression. d) Kaplan-Meier survival analysis in lung cancer patients ( $n = 994$ ) indicates that high MCT1 expression correlates with poorer patient survival ( $p < 0.05$ ). e) Kaplan-Meier survival analysis in lung cancer patients indicates that high LDHA expression correlates with poorer patient survival ( $p < 0.0001$ ). f) Mosaic plot in lung



cancer patients indicates that MCT1 expression correlates with LDHA expression ( $p < 0.0001$ ). g) Kaplan-Meier survival analysis in cervical cancer patients ( $n = 291$ ) indicates that high MCT1 expression correlates with poorer patient survival ( $p < 0.0001$ ). h) Kaplan-Meier survival analysis in cervical cancer patients indicates that high LDHA expression correlates with poorer patient survival ( $p < 0.001$ ). i) Mosaic plot in cervical cancer patients indicates that MCT1 expression correlates with LDHA expression ( $p < 0.0001$ ).

## Reference

1. Zacharias NM, *et al.* (2019) Assessing metabolic intervention with a glutaminase inhibitor in real-time by hyperpolarized magnetic resonance in acute myeloid leukemia. *Mol Cancer Ther* 18(11):1937-1946.
2. Miller JJ, *et al.* (2018) <sup>13</sup>C pyruvate transport across the blood-brain barrier in preclinical hyperpolarised MRI. *Sci Rep* 8(1):15082.